

Spin photonics and spin-photonic devices with dielectric metasurfaces

Yachao Liu, Shizhen Chen, Yougang Ke, Xinxing Zhou, Hailu Luo*, and Shuangchun Wen
 Laboratory for Spin Photonics, School of Physics and Electronics, Hunan University,
 Changsha 410082, China

ABSTRACT

Dielectric metasurfaces with spatially varying birefringence and high transmission efficiency can exhibit exceptional abilities for controlling the photonic spin states. We present here some of our works on spin photonics and spin-photonic devices with metasurfaces. We develop a hybrid-order Poincaré sphere to describe the evolution of spin states of wave propagation in the metasurface. Both the Berry curvature and the Pancharatnam-Berry phase on the hybrid-order Poincaré sphere are demonstrated to be proportional to the variation of total angular momentum. Based on the spin-dependent property of Pancharatnam-Berry phase, we find that the photonic spin Hall effect can be observed when breaking the rotational symmetry of metasurfaces. Moreover, we show that the dielectric metasurfaces can provide great flexibility in the design of novel spin-photonic devices such as spin filter and spin-dependent beam splitter.

Keywords: photonic spin Hall effect, metasurfaces, spin photonics, Poincaré sphere

1. INTRODUCTION

Spin provides a reliable degree of freedom for light control and optical data storage.¹⁻⁴ To employ this degree of freedom, an effective method for spin-orbital coupling is required in the light-matter interaction. This coupling will lead to a featured spin dependent response in optical materials or in the emerging fields. For particular responses, it can be applied for different uses such as the spin-controlled plasmonic transmission and the spin dependent beam steering.^{5,6} To design the electromagnetic response, many material systems have been studied in recent years.^{7,8} The phase gradient metasurfaces have been verified as a giant photonic spin Hall effect (SHE) generator.² Quantum dots and nitrogen-vacancy centers in diamond are believed as the candidates for quantum interface between stationary and flying qubits.⁹ Also such as the plasmonic structures be designed for the near-field vortex mode generation and the polarization sensitive focusing.^{10,11}

Metasurfaces can artificially design the spin-dependent or the orbital-relevant responses of the emerging field, thus is a promising route to mould the light.^{2,3,8,12,13} The dispersion engineering of metasurfaces can be realized by changing the material compositions, the pattern of local components, and the arrangement of these local patterns.¹⁴⁻¹⁶ The flexible designing and reduced dimension of metasurfaces make it potentially a wonderful candidate for the on-chip optics and the integrated optics.¹⁷⁻¹⁹ To achieve a spin-dependent behavior, the comprising sub-wavelength structures must be polarization (spin) sensitive. The polarization (spin) related evolving process of light is affirmatively to impose a geometric phase into the light, which is usually called Pancharatnam-Berry (PB) phase.^{10,20,21} There is therefore a strong motivation to peer into the spin-dependent PB phase for exploring the applications of metasurface in spin photonics.

In the paper, we reviewed some of our works on the spin photonics and spin photonic devices base on the dielectric metasurfaces. The Poincaré sphere is an intuitive tool to understand the polarization (spin) and spatial optical mode evolving process.²²⁻²⁵ We developed a hybrid-order Poincaré sphere to describe the evolution of polarization states of wave propagation in inhomogeneous anisotropic media.²⁶ And the dielectric metasurfaces are applied to show examples of this evolutions.^{27,28} Furthermore, the dielectric metasurfaces can dramatically reduce the losses induced in the propagation,²⁹ which limited the practical application of metamaterials since

*Hailu Luo email address: hailuluo@hnu.edu.cn

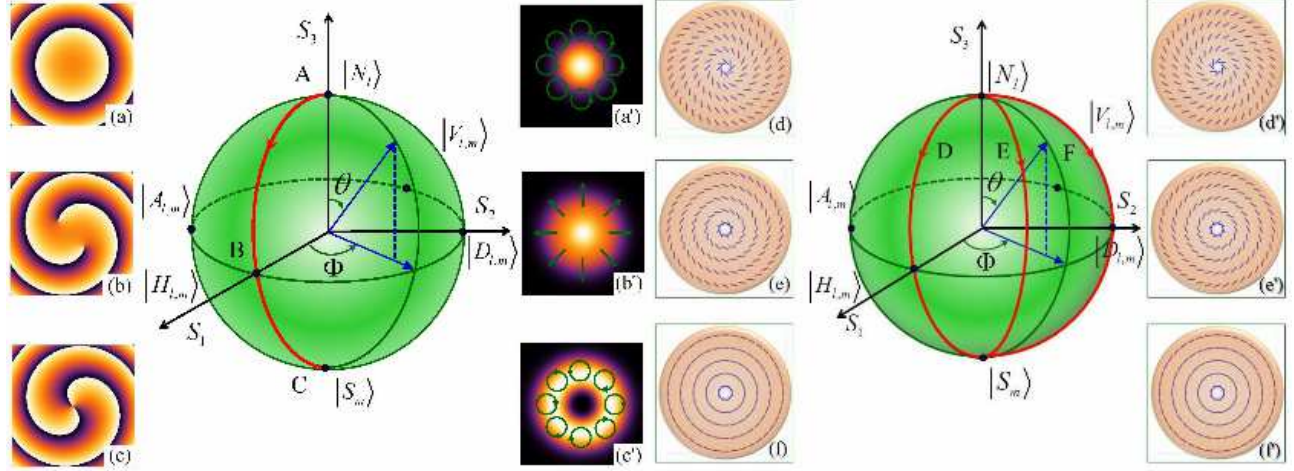


Figure 1. The left schematic illustration shows the evolution of phase and polarization on hybrid-order Poincaré sphere. The sphere is assumed with state $\sigma = +1$ and $l = 0$ in the north pole, and the state $\sigma = -1$ and $m = +2$ in the south pole. Insets (a)-(c) show the phase for points A, B, and C, respectively. Insets (a')-(c') show the polarization state of these points respectively. The right schematic illustration shows realization of the evolution along different longitude lines on the hybrid-order Poincaré sphere ($l = 0$ and $m = -2$). By choosing the initial spin state σ and the initial angle α_0 of the dielectric metasurfaces, we can change the evolving longitudes. Insets (d)-(f) are the evolutions along the longitude lines D, E, and F from the north pole to south pole, respectively. While, insets (d')-(f') are the evolutions along the longitude lines D, E, and F from south pole to north pole. The initial angle of metasurfaces can be obtained by the relation $\Phi = 2\alpha_0 - \pi/2$ from the north pole to south pole, and $\Phi = 2\alpha_0 + \pi/2$ from the south pole to north pole.²⁶

its advent. Therefore, the dielectric metasurfaces are expected to be alternative in the integrated optics. We provided some schemes base on the dielectric metasurfaces to realize the giant photonic SHE generator, mode splitter, and spin filter. The rest of the paper is organized as follows. In Sec. 2, we establish a hybrid-order Poincaré sphere model to describe the complicate evolutions of polarization and deduce the involved PB phases. Moreover, we introduce the precondition for the photonic SHE caused by PB phase in the dielectric metasurfaces. In the Sec. 3, some spin-photonics devices based on the dielectric metasurfaces are demonstrated. Finally, a conclusion is given in Sec. 4.

2. HYBRID-ORDER POINCARÉ SPHERE

Polarization and phase are two intrinsic features of electromagnetic waves. To describe the fundamental homogeneous polarization states, a prominent geometric representation known as the Poincaré sphere was proposed in 1892, in which the homogeneous polarization states are mapped to the surface of a unit sphere through the Stokes parameters in the sphere's Cartesian coordinates.²² Analogue to this geometric representation of polarization, the orbital Poincaré sphere was proposed to describe the spatial mode of beam in recent, in which each point on the unit spherical surface represents a unique spatial mode of the same order.²³ Both of these representations provide a intuitive way to treat the complicated phenomena with varying states. It is well known that the cyclic transformation of a light beam will endow the light an additional geometric phase. Therefore, the Poincaré sphere representations are definitely efficient approaches to find these additional phases.

However, the researches of spatial inhomogeneous polarization states have broken through the limit of general Poincaré sphere recently. For example, cylindrical vector beam refers to the polarization state with cylindrical symmetry,³⁰ which attracted significant attentions because of their unique properties under high-numerical-aperture focusing.^{31,32} To demonstrate the transformation of these higher-order solutions of Maxwells equations, the high-order Poincaré sphere has been developed in the most recent.^{24,25} The north and south poles of the high-order Poincaré sphere represent the opposite spin states and orbital states. Any states on the high-order Poincaré sphere, can be realized by a superposition of the two orthogonal states. The same as the cyclic evolution

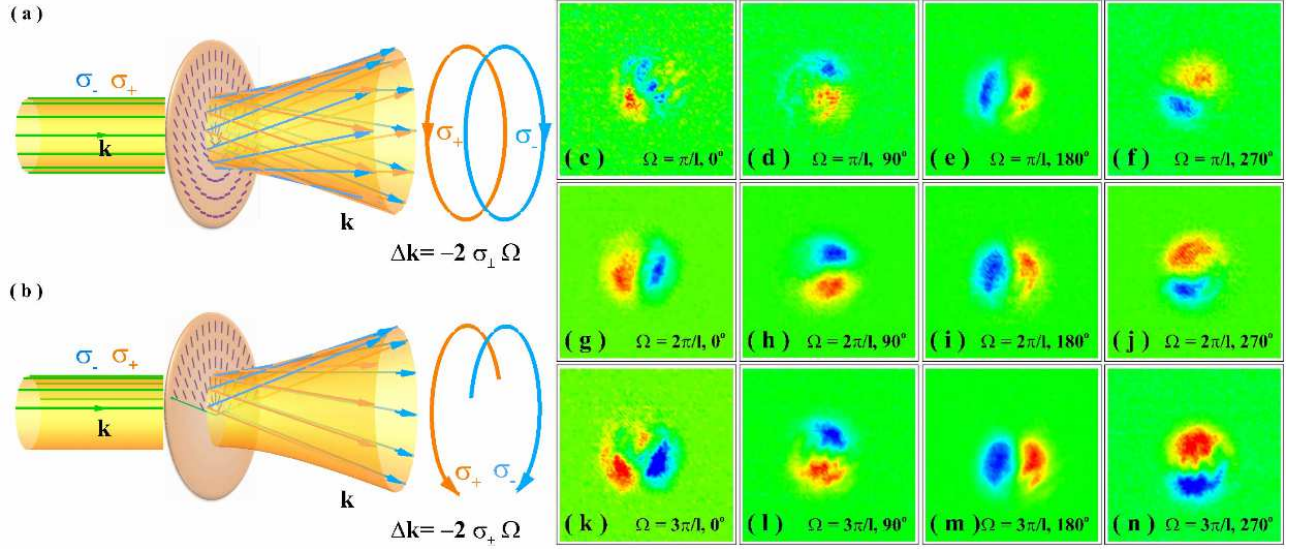


Figure 2. (a)-(b) Contrast between the metasurfaces (a) with rotational symmetry and (b) with rotational symmetry breaking. The rotational symmetry can be broken by designing the structure of the metasurface, which just maintains part of the inner structure (b) comparing with the metasurface with rotational symmetry (a), or by displacing the incident beam from the central axis of the metasurface. The notations σ_+ and σ_- represent left- and right-spin states, respectively, and Ω is rotation rate of the metasurface. (c)-(n) The S3 results of photonic SHE when we break the rotational symmetry of PB phase; red and blue represent the left and right-circular spin states, respectively. The three rows correspond to the results of three different metasurfaces measured in four different positions $\Psi = 0^\circ, 90^\circ, 180^\circ, \text{ and } 270^\circ$.³⁵

of fundamental polarization state will lead to an additional phase, which is named as the PB phase, the higher-order polarization state evolution will also lead to a higher-order PB phase.³³

Nevertheless, all the above solutions can not describe the polarization transforms from a homogeneous state to a higher-order state. These cases are usually involved in the inhomogeneous anisotropic media interactions.³⁴ To address this concern, we present a hybrid-order Poincaré sphere to demonstrate the more comprehensive evolution of polarization and phase.²⁶ In the constructed parameter space, all the states of hybrid-order Poincaré sphere is given by

$$|\psi(\theta, \Phi)\rangle = \cos \frac{\theta}{2} |\mathbf{N}_l\rangle + \sin \frac{\theta}{2} |\mathbf{S}_m\rangle \exp(+i\sigma\Phi), \quad (1)$$

where $|\mathbf{N}_l\rangle = \frac{\sqrt{2}}{2}(\mathbf{e}_x + i\sigma\mathbf{e}_y) \exp(il\Phi/2)$, and $|\mathbf{S}_m\rangle = \frac{\sqrt{2}}{2}(\mathbf{e}_x - i\sigma\mathbf{e}_y) \exp(im\Phi/2)$ are polarization and phase states represented by the poles. The coordinates (θ, Φ) are respectively the latitude and longitude on the sphere. The optical spin angular momentum (SAM) of a photon is $\sigma\hbar$ ($\sigma = \pm 1$), \hbar is the reduced Plank constant; the azimuthal phase factor $\exp(il\Phi)$ is a phase vortex, the optical orbital angular momentum (OAM) eigenstates of a photon is $lh/m\hbar$ ($l, m = 0, \pm 1, \pm 2 \dots$), l/m is the topological charge; and $(\mathbf{e}_x \pm i\sigma\mathbf{e}_y)$ is right or left circular polarization depending on the spin of photon σ . Figure 1 schematically shows the idea of hybrid-order Poincaré sphere.

It is worth noting that the hybrid-order Poincaré sphere has two special features in comparing with the high-order Poincaré sphere: (1) The orbital states on the hybrid-order Poincaré sphere should not be confined to have the same values and opposite signs. As a result, the cylindrical vector vortex beams can be represented by the equatorial points. Intermediate points between the poles and equator represent the elliptically polarized vector vortex beams. (2) Polarization and phase evolution in any metasurfaces with cylindrically symmetrical optical axis distribution can be conveniently described by state evolution along the longitude line on the hybrid-order Poincaré sphere. Therefore, the hybrid-order Poincaré sphere is a predictable way to access the PB phase involved in the optical transform inside an inhomogeneous anisotropic medium. The dielectric metasurface is expected to be a good candidate for realizing the evolution of polarization states on the hybrid Poincaré sphere.

By correctly controlling the local orientation and geometrical parameters of the nanograting, one can achieve any desired polarization distributions on the hybrid-order Poincaré sphere, as the right picture of Fig. 1 showing.

To get the PB phase, we deduced the Berry connection and the Berry curvature when the states evolve on the surface of the hybrid-order Poincaré sphere. The Berry connection can be written as

$$\mathbf{A} = i\langle\psi(\mathbf{R})|\nabla_{\mathbf{R}}|\psi(\mathbf{R})\rangle. \quad (2)$$

Where $\mathbf{R} = (\rho, \theta, \Phi)$ is the coordinate in parameter space. After substituting, we find the only nonzero component of Berry connection in our case:

$$\mathbf{A}_{\Phi} = -\frac{1}{4\rho\sin\theta}[l(1 + \cos\theta) + (m + 2\sigma)(1 + \cos\theta)]. \quad (3)$$

Then we get the Berry curvature $\mathbf{V}(\mathbf{R})$ and PB phase $\gamma(C)$ in hybrid-order Poincaré sphere:

$$\mathbf{V}(\mathbf{R}) = -\nabla_{\mathbf{R}} \times \mathbf{A} = \frac{l - (m + 2\sigma)}{4\rho^2} \hat{\rho}, \quad (4)$$

$$\gamma(C) = -\int \int_C d\mathbf{S} \cdot \mathbf{V}(\mathbf{R}) = -\frac{l - (m + 2\sigma)}{4} \Theta, \quad (5)$$

where $d\mathbf{S} = \rho^2 \sin\theta d\rho d\theta d\Phi \hat{\rho}$, C is the route of a cyclic transformation in parameter space \mathbf{R} , Θ is the surface area on the hybrid-order Poincaré sphere enclosed by the circuit C .

The PB phase is immanent in the spin-orbit interaction (SOI) processes with polarization varying, which may lead to the photonic SHE. However, the precondition for observing this photonic SHE is still obfuscated. We present that it is necessary to break the rotational symmetry of metasurface for the emergence of photonic SHE in the momentum space.³⁵ The dielectric metasurfaces are chosen as the examples to demonstrate our deduction. When the phase retardances are fixed at π , the metasurfaces can be viewed as the a spatially variant half-waveplate. It is well known that the half-waveplate will convert the chirality of circularly polarized beams, which lead to the evolution of states along the longitudes of Poincaré sphere. Thus the process will endow the light an additional PB phase. From the Eq. (5), it can be deduced that the PB phase equals half of the surface area enclosed by the evolution route C , where l and m both equal zero for these localized situations. Furthermore, the evolving longitudes are decided by the orientation of optical axes ϕ of the inhomogeneous half-waveplate and the sign of PB phase is decided by the incident polarization state σ . By this way, a spatially variant phase distribution can be induced by engineering the orientations of local optical axes.

A metasurface with rotational symmetry is designed in our work, as shown in Fig 2(a). It is well known that the phase variation across the beam would deflect the light $\Delta\mathbf{k} = \nabla\Phi$ (\mathbf{k} is the wave vector). Note that the geometric phase gradient in the azimuthal direction is proportional to the rotation rate of local optical axes $\Omega = d\phi/dx$, and that it is spin-dependent in sign but equal in magnitude. When we refer to a small part of the metasurface as the input light isn't located at the center of the metasurface, the phase gradient can be approximately regarded as in one dimension (x). Thus, the constructed geometric phase gradient can be related to the rotation rate of local optical axes in the form:

$$\Delta_x \mathbf{k} = \nabla_x \Phi = d\Phi/dx = \frac{\sigma_{\pm} 2d\phi}{dx} = 2\sigma_{\pm} \Omega, \quad (6)$$

where Φ is the induced PB phase. Thus, when the metasurface is engineered with rotational symmetry, the induced PB phase gradient would deflect the light along the azimuth dimension.

However, the deflections of different spin components are opposite as the PB phase is spin-dependent. Therefore, the wave vectors of the two spin components are still interlaced after passing the metasurface, thus no spin-dependent splitting in position space occurs. By breaking the rotational symmetry of the metasurface, the kept part of the metasurface can still deflect the light, but the wave vectors cannot be still interlaced after propagation, as shown in Fig 2(b). By this way, we observed the photonic SHE in our experiments. Furthermore, we

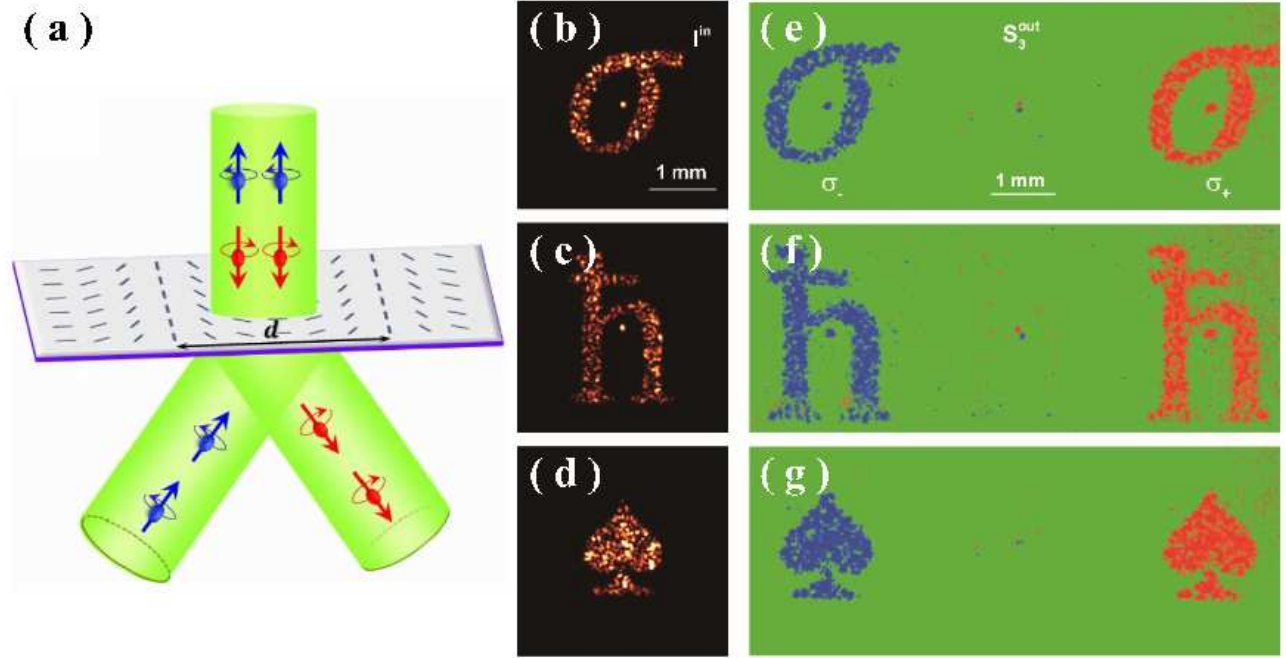


Figure 3. (a) Schematic illustration of spin-dependent splitting. The small balls with arrows represent the left- (red) and right-handed (blue) photons, respectively. The metasurface reverses the chirality of incident photons and steers normally incident photons with opposite handedness to two directions, due to space-variant PBP varying in one dimension. (b)-(d) Intensity patterns (middle column) of three typical linear polarization beams (two spin-dependent letters σ and h and one symbol \spadesuit in the order from top to bottom) before the dielectric metasurface. (e)-(g) The corresponding spin-dependent splitting patterns after the dielectric metasurface are discriminated by the normalized Stokes parameter S_3 (right column).

reported the observation of photonic SHE near the phase singularity at dielectric metasurfaces.³⁶ The rotationally arranged structures (structure parameter q) are applied in this experiment. For a linearly polarized incident vortex beam (topological charge l), the spin-orbit coupling of light in the metasurface will lead to the appearance of the helical phase with topological charge $\pm 2q$ for the opposite spin components respectively. Therefore, the superposition of the induced PB phase and the original vortex phase $l \pm 2q$ will eliminate the phase singularity of one spin component ($l - 2q = 0$ or $l + 2q = 0$), while enhances the phase singularity of the other. By switching the signs of the topological charges of the input beam, the spin-dependent splitting pattern can be manipulated effectively.

Moreover, there is still not an effective method to generate all the states on higher-order Poincaré sphere and realize the state evolution. Most efforts have been made to obtain the radial and azimuthal polarized beams, but the other states are seldom referred to. We provided two feasible schemes to fill this blank. The first one is based on the superposition of two orthogonal circularly polarized vortex beams, where the chirality of the two vortex beams are also opposite. A modified Mach-Zender interferometer is applied to make the superposition and finally construct the arbitrary cylindrical vector beams on the higher-order Poincaré sphere.³⁷ For more simplicity, a dielectric metasurface was designed to realize this purpose.²⁷ By just adjusting the incident fundamental polarization state, we can access arbitrary states on higher-order Poincaré sphere. Furthermore, by simply rotating a polarizer or a quarter waveplate in our setup, the produced state will evolve along the latitude or longitude of the higher-order Poincaré sphere. Moreover, a versatile scheme based on two cascaded metasurfaces is proposed to acquire arbitrary linearly polarized vector vortex states, which are the particular points of the higher-order Poincaré sphere and the hybrid-order Poincaré sphere.²⁸

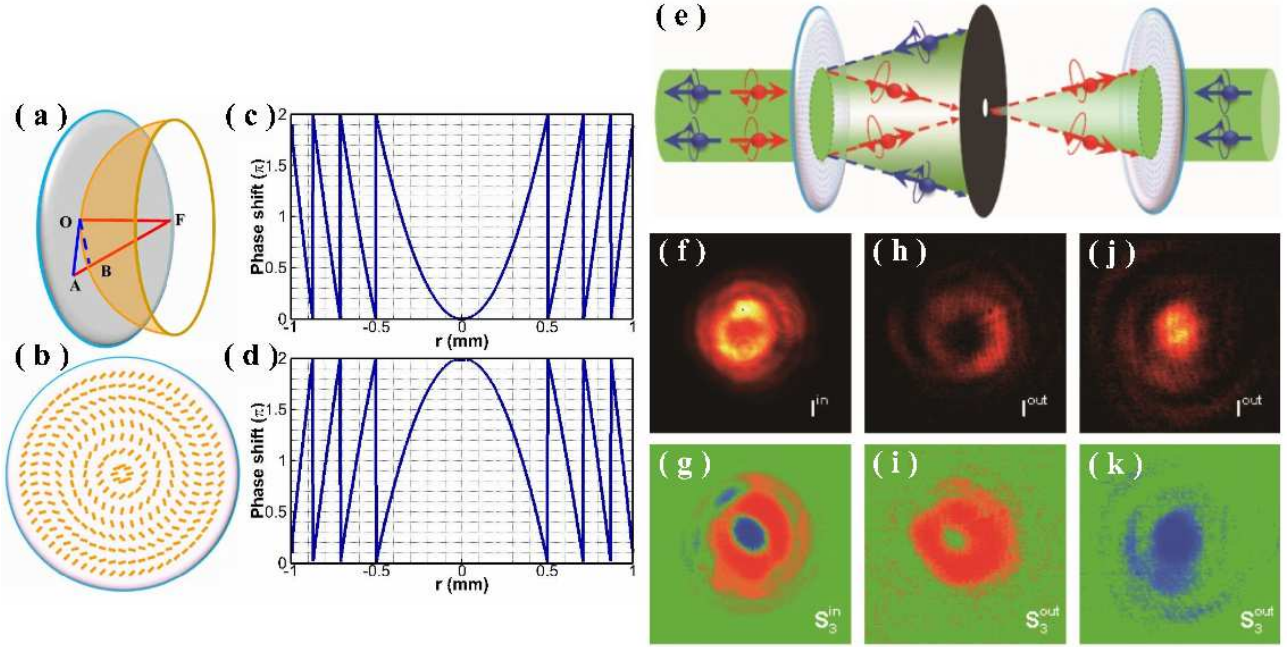


Figure 4. (a) The schematic illustration of a metasurface lens with focal distance f and the theoretical hyperboloidal equiphase surface of this focusing lens. (b) The optical axis distribution of a left-handed circular polarized plane wave focusing lens. (c)-(d) The phase shift introduced by the same metasurface from the identical incident plane, for left-handed circular polarization and right-handed circular polarization beam incidence, respectively. (e) Schematic setup for the photonic spin filter. The small balls with arrows represent the left- (red) and right-handed (blue) photons, respectively. The first metasurface reverses the chirality of incident photons and results in the focusing of a selected spin component, a diaphragm located at co-focus plane of the two metasurfaces blocks the divergent spin component but releases the selected one. Finally, another metasurface recovers the original spin state and propagation direction of the emerging photons. (f) and (g) show the intensity and normalized Stokes parameter S_3 of incident beam with the superposition of right-handed circularly polarized plane Gaussian beam and left-handed circularly polarized Laguerre-Gaussian beam with topological charge 1. (h) and (i) are respectively the intensity distribution and normalized Stokes parameter S_3 of the emerging beam of right-handed filter (blocking the right-hand photons and releasing the left-hand photons). (j) and (k) are the contrary results for the left-handed filter (blocking the right-hand photons and releasing the left-hand photons).

3. SPIN-PHOTONIC DEVICES

In spite of the huge efforts devoted in the recent years, the practical application of metal metamaterials/metasurfaces is still restricted, as the limited high device efficiencies caused by the Ohmic losses in the metal and the limited scattering cross sections of the micro-elements.^{38,39} However, owing to the comparatively small losses in the optical range, dielectric metasurfaces provide the possibilities to realize the practically high quality transmission-type optical devices, which is desperate for the integrate optics.^{29,40,41} Here, we report a giant photonic SHE generator, a spin-dependent beam splitter, and a spin filter based on the dielectric metasurfaces. The transparent dielectric materials is the guarantee of high transmit efficiency, and the orientation related geometric PB phase design makes it function-customizable for these dielectric metasurfaces.

As the photonic counterpart of electronic SHE, photonic SHE is a rising star in recent years with high expectations in the precise metrology, light manipulation, quantum communication, and quantum computation.^{2,3,42-46} Actually, this effect is the outcome of the mutual influence between the photon spin (polarization) and the trajectory (orbital angular momentum) of light-beam propagation, i.e., SOI.^{1,10,20,47} Thus the photonic SHE is sensitive to the external disturbances, including the material permittivity, dynamic shift, and ambient temperature. Nonetheless, it is difficult to retrieve this variation by measuring the photonic SHE. There is an exceptional difficult to detect this effect directly, as the original SOI is generally very weak. A precise but complex method dubbed quantum weak measurement is developed in the past decade to detect the tiny spin-dependent shift which is the manifestation of photonic SHE.^{42,48,49} Meanwhile, it is also profound to find a controllable and directly

measurable photonic SHE for the practical applications. We reported a giant photonic SHE generator in momentum space based on the dielectric metasurface.⁵⁰ In our scenario, the PB phase gradient induces a constant momentum shift, i.e., a spin-dependent angular deflection. The angular deflection in real-space is well-known that increases linearly with the propagation distance. In addition, this angular deflection is proportional to the rotation rate of the metamaterial, and that the direction of spin shift can be reversed by changing the sign of rotation rate. While the rotation rate can be tuned by modulating the structural geometry of the metamaterial. Based on the Eq. (6), we get the splitting of light:

$$\Delta x = (\Delta \mathbf{k} / \mathbf{k}_0) z = (2\sigma_{\pm} \Omega / \mathbf{k}_0) z, \quad (7)$$

where $\mathbf{k}_0 = 2\pi/\lambda_0$, λ_0 is the wavelength of incident light, z is the propagation distance. In compare with the photonic SHE that occurs in the interfacial reflection and refraction, which exhibits a constant beam shift limited to a fraction of the wavelength, the spin-dependent shift induced in our scheme is sufficiently large to allow for direct measurement. Therefore, such a structured metamaterial offers an additional degree of freedom for the manipulation of the photonic SHE, especially in the effort to obtain a giant photonic SHE.

Polarizing beam splitters which can separate the two orthogonal polarizations of light beam into different propagation directions, are widely used in optical communications, imaging systems, and optical recording. Conventional polarizing beam splitters made by naturally anisotropic materials require a large thickness to generate the enough walk-off distance between the two orthogonal polarizations, owing to the intrinsically small birefringence. However, it is still a challenge to realize the circular polarization beam splitter due to the lack of natural materials with sufficient circular birefringence. Recently, benefitting from the prosperity of artificial materials in the nearest researches, including metamaterials, plasmonic metasurfaces, and the materials designed in transform optics, many novel schemes are proposed for the realization of beam splitters with special characteristics. Here, we demonstrate a circular polarization beam splitter base on the PB phase dielectric metasurface. As illustrated in Fig. 3, the metasurface separates the normally incident light to two distinct parts with opposite helicities due to the engineered PB phase gradient. The same as what we have mentioned above, the linearly rotated local optical axes in dielectric metasurfaces will introduce a spin dependent phase gradient at the beam transverse section. Therefore, circularly polarized beams will be separated according to their polarization. By this way, the light beam encoded with arbitrary intensity patterns can be separated after passing through the metasurface spin splitter, and that the splitting angle can be adjusted according to the Eq. (7). Figures 3(e)-3(g) exhibit the observed splitting results in our experiment.

Spin of photon provides a new degree of freedom to control light, and enables many new spin-based applications. The spin filter which screens out the pure spin photons is essential for the application of this degree of freedom, similar to those in the spintronics. We reports the experimental demonstration of the photon spin filter based on two cascaded metasurfaces which is constructed with the varying local optical axes in the radial direction. Firstly, a dielectric metasurface lens is designed as shown in Fig. 4(a). By locally adjusting the optical axis orientations, as the Fig. 4(b) showing, the induced PB phases for the opposite spin components are distributed as the Fig. 4(c) and Fig. 4(c) showing. It is clear that the PB phases will focus the left-hand circularly polarized component while diverge the right-hand component. Therefore, based on the cascaded metasurface lenses and a diaphragm, we obtain a optical spin filter. As shown in Fig. 4(e), the first metasurface reverses the chirality of incident photons and imposes a PB phase on the incident light, thus resulting in a spin-dependent expansion or focus for the opposite spin components of light. The focused photons then pass through a diaphragm and the unwanted spin component is blocked. Another metasurface is employed to recover the spin state and propagation direction of the selected component. Figures 4(f)- 4(k) exhibit the ability of this spin-filter, normally incident photons with right-handed (left-handed) spin are almost totally blocked, whereas normally incident photons with lefthanded (right-handed) spin are almost totally transmitted. To distinguish the opposite spin components, a fundamental Gaussian mode is endowed to the left-hand spin component, and a Laguerre-Gaussian mode is endowed to the right-hand component. The passing spin component can be reversed by engineering the metasurface with an opposite spatial rotation rate.

4. CONCLUSIONS

In summary, we have reviewed our recent works on spin photonics and Spin-photonic devices with dielectric metasurfaces. The coupling between a photon's spin state with its orbit degree of freedom is known as the

spin-orbit interaction, which contributes to two types of geometric phase: the Rytov-Vladimirskii-Berry phase and the Pancharatnam-Berry phase. The former is associated to the evolution of propagation direction of light and the latter to the variation of polarization state. It is feasible to manipulate the polarization and propagation rule of light by designing the geometric phase. However, the majority of traditional plasmonic metasurfaces are based on the RVB phase or on the PB phase but being restricted to near field. Dielectric metasurfaces fabricated of transparent materials constitute a class of metasurface with considerable flexibility in the manipulation of geometric phase and with high transmission efficiency. We present here some of our works on applying the dielectric metasurfaces to realize the evolution of polarization states on Poincaré sphere and the manipulation of propagation rule of light, moreover, we show that the dielectric metasurfaces can develop novel spin-photonic devices such as spin filter and spin-dependent beam splitter. It is the high transmission efficiency of dielectric metasurfaces makes it possible to utilizing the spin-dependent effect based on PB phase in optical far field, which would substantially facilitate the development of spin-dependent devices in photonics.

ACKNOWLEDGMENTS

This research was partially supported by the National Natural Science Foundation of China (Grants Nos. 11274106 and 11474089).

REFERENCES

1. M. Onoda, S. Murakami, and N. Nagaosa, “Hall effect of light,” *Phys. Rev. Lett.* **93**, 083901 (2004).
2. X. Yin, Z. Ye, J. Rho, Y. Wang, and X. Zhang, “Photonic spin Hall effect at metasurfaces,” *Science* **339**, 1405 (2013).
3. N. Shitrit, I. Yulevich, E. Maguid, D. Ozeri, D. Veksler, V. Kleiner, and E. Hasman, “Spin-optical metamaterial route to spin-controlled photonics,” *Science* **340**, 724 (2013).
4. K. Y. Bliokh, D. Smirnova, and F. Nori, “Quantum spin Hall effect of light,” *Science* **348**, 1148 (2015).
5. J. Lin, J. P. B. Mueller, Q. Wang, G. Yuan, N. Antoniou, X. Yuan, and F. Capasso, “Polarization-controlled tunable directional coupling of surface plasmon polaritons,” *Science* **340**, 331 (2013).
6. L. Huang, X. Chen, B. Bai, Q. Tan, G. Jin, T. Zentgraf, and S. Zhang, “Helicity dependent directional surface plasmon polariton excitation using a metasurface with interfacial phase discontinuity,” *Light Sci. Appl.* **2**, e70 (2013).
7. N. M. Litchinitser, “Structured light meets structured matter,” *Science* **337**, 1054 (2012).
8. A. V. Kildishev, A. Boltasseva, and V. M. Shalaev, “Planar photonics with metasurfaces,” *Science* **339**, 1232009 (2013).
9. W. B. Gao, P. Fallahi, E. Togan, J. Miguel-Sanchez, and A. Imamoglu, “Observation of entanglement between a quantum dot spin and a single photon,” *Nature* **491**, 426 (2012).
10. K. Y. Bliokh, Y. Gorodetski, V. Kleiner, and E. Hasman, “Coriolis effect in optics: unified geometric phase and spin-Hall effect,” *Phys. Rev. Lett.* **101**, 030404 (2008).
11. Y. Gorodetski, A. Niv, V. Kleiner, and E. Hasman, “Observation of the spin-based plasmonic effect in nanoscale structures,” *Phys. Rev. Lett.* **101**, 043903 (2008).
12. N. Yu and F. Capasso, “Flat optics with designer metasurfaces,” *Nat. Mater.* **13**, 139 (2013).
13. N. Meinzer, W. L. Barnes, and I. R. Hooper, “Plasmonic meta-atoms and metasurfaces,” *Nature Photon.* **8**, 889 (2014).
14. N. Yu, P. Genevet, M. A. Kats, F. Aieta, J. Tetienne, F. Capasso, and Z. Gaburro, “Light propagation with phase discontinuities: generalized laws of reflection and refraction,” *Science* **334**, 333 (2011).
15. L. Huang, X. Chen, H. Mühlenbernd, G. Li, B. Bai, Q. Tan, G. Jin, T. Zentgraf, and S. Zhang, “Dispersionless phase discontinuities for controlling light propagation,” *Nano Lett.* **12**, 5750 (2012).
16. P. Genevet, N. Yu, F. Aieta, J. Lin, M. A. Kats, R. Blanchard, M. O. Scully, Z. Gaburro, and F. Capasso, “Ultrathin plasmonic optical vortex plate based on phase discontinuities,” *Appl. Phys. Lett.* **100**, 013101 (2012).
17. S. Sun, Q. He, S. Xiao, Q. Xu, X. Li, and L. Zhou, “Gradient-index meta-surfaces as a bridge linking propagating waves and surface waves nature mater,” *Nature Mater.* **11**, 426 (2012).

18. X. Ni, A. V. Kildishev, and V. M. Shalaev, "Metasurface holograms for visible light," *Nat. Commun.* **4**, 2807 (2013).
19. Y. Liu and X. Zhang, "Metasurfaces for manipulating surface plasmons," *Appl. Phys. Lett.* **103**, 141101 (2013).
20. K. Y. Bliokh, A. Niv, V. Kleiner, and E. Hasman, "Geometrodynamics of spinning light," *Nature Photon.* **2**, 748 (2008).
21. X. Ding, F. Monticone, K. Zhang, L. Zhang, D. Gao, S. N. Burokur, A. de Lustrac, Q. Wu, C. Qiu, and A. Alù, "Ultrathin Pancharatnam-Berry metasurface with maximal cross-polarization efficiency," *Adv. Mater.* **27**, 1195 (2015).
22. H. Poincaré, *Theorie Mathématique de la Lumière* (GauthiersVillars, Paris, 1892).
23. M. J. Padgett and J. Courtial, "Poincaré-sphere equivalent for light beams containing orbital angular momentum," *Opt. Lett.* **24**, 430 (1999).
24. G. Milione, H. I. Sztul, D. A. Nolan, and R. R. Alfano, "Higher-order Poincaré sphere, Stokes parameters, and the angular momentum of light," *Phys. Rev. Lett.* **107**, 053601 (2011).
25. A. Holleccek, A. Aiello, C. Gabriel, C. Marquardt, and G. Leuchs, "Classical and quantum properties of cylindrically polarized states of light," *Opt. Express* **19**, 9714 (2011).
26. X. Yi, Y. Liu, X. Ling, X. Zhou, Y. Ke, H. Luo, S. Wen, and D. Fan, "Hybrid-order Poincaré sphere," *Phys. Rev. A* **91**, 023801 (2015).
27. Y. Liu, X. Ling, X. Yi, X. Zhou, H. Luo, and S. Wen, "Realization of polarization evolution on higher-order Poincaré sphere with metasurface," *Appl. Phys. Lett.* **104**, 191110 (2014).
28. X. Yi, X. Ling, Z. Zhang, X. Zhou, Y. Liu, S. Chen, H. Luo, and S. Wen, "Generation of cylindrical vector vortex beams by two cascaded metasurfaces," *Opt. Express* **22**, 17207 (2014).
29. D. Lin, P. Fan, E. Hasman, and M. L. Brongersma, "Dielectric gradient metasurface optical elements," *Science* **345**, 298 (2014).
30. Q. Zhan, "Cylindrical vector beams: from mathematical concepts to applications," *Adv. Opt. Photonics* **1**, 1-57 (2009).
31. L. Novotny, M. R. Beversluis, K. S. Youngworth, and T. G. Brown, "Longitudinal field modes probed by single molecules," *Phys. Rev. Lett.* **86**, 5251 (2001).
32. R. Dorn, S. Quabis, and G. Leuchs, "Sharper focus for a radially polarized light beam," *Phys. Rev. Lett.* **91**, 233901 (2003).
33. G. Milione, S. Evans, D. A. Nolan, and R. R. Alfano, "Higher order Pancharatnam-Berry phase and the angular momentum of light," *Phys. Rev. Lett.* **108**, 190401 (2012).
34. L. Marrucci, C. Manzo, and D. Paparo, "Optical spin-to-orbital angular momentum conversion in inhomogeneous anisotropic media," *Phys. Rev. Lett.* **96**, 163905 (2006).
35. Y. Liu, X. Ling, X. Yi, X. Zhou, S. Chen, Y. Ke, H. Luo, and S. Wen, "Photonic spin Hall effect in dielectric metasurfaces with rotational symmetry breaking," *Opt. Lett.* **40**, 756 (2015).
36. Y. Li, Y. Liu, X. Ling, X. Yi, X. Zhou, Y. Ke, H. Luo, S. Wen, and D. Fan, "Observation of photonic spin Hall effect with phase singularity at dielectric metasurfaces," *Opt. Express* **23**, 1767 (2015).
37. S. Chen, X. Zhou, Y. Liu, X. Ling, H. Luo, and S. Wen, "Generation of arbitrary cylindrical vector beams on the higher order Poincaré sphere," *Opt. Lett.* **39**, 5274 (2014).
38. S. Sun, K. Yang, C. Wang, T. Juan, W. T. Chen, C. Y. Liao, Q. He, S. Xiao, W. Kung, G. Guo, Lei Zhou, and D. P. Tsai, "High-efficiency broadband anomalous reflection by gradient meta-surfaces," *Nano Lett.* **12**, 6223 (2012).
39. A. Pors, O. Albrektsen, I. P. Radko, and S. I. Bozhevolnyi, "Gap plasmon-based metasurfaces for total control of reflected light," *Sci. Rep.* **3**, 2155 (2013).
40. D. Hakobyan and E. Brasselet, "Left-handed optical radiation torque," *Nat. Photonics* **8**, 610 (2014).
41. P. R. West, J. L. Stewart, A. V. Kildishev, V. M. Shalaev, V. V. Shkunov, F. Strohkendl, Y. A. Zakharenkov, R. K. Dodds, and R. Byren, "All-dielectric subwavelength metasurface focusing lens," *Opt. Express* **22**, 26212 (2014).
42. O. Hosten and P. Kwiat, "Observation of the spin Hall effect of light via weak measurements," *Science* **319**, 787 (2008).

43. G. Li, M. Kang, S. Chen, S. Zhang, E. Y. Pun, K. W. Cheah, and J. Li. "Spin-enabled plasmonic metasurfaces for manipulating orbital angular momentum of light," *Nano Lett.* **13**, 4148 (2013).
44. X. Zhou, Z. Xiao, H. Luo, and S. Wen, "Experimental observation of the spin Hall effect of light on a nanometal film via weak measurements," *Phys. Rev. A* **85**, 043809 (2012).
45. X. Zhou, X. Ling, H. Luo, and S. Wen, "Identifying graphene layers via spin Hall effect of light," *Appl. Phys. Lett.* **101**, 251602 (2012).
46. X. Zhou, J. Zhang, X. Ling, S. Chen, H. Luo, and S. Wen, "Photonic spin Hall effect in topological insulators," *Phys. Rev. A* **88**, 053840 (2013).
47. K. Y. Bliokh and Y. P. Bliokh, "Conservation of angular momentum, transverse shift, and spin Hall effect in reflection and refraction of an electromagnetic wave packet," *Phys. Rev. Lett.* **96**, 073903 (2006).
48. Y. Qin, Y. Li, H. He, and Q. Gong, "Measurement of spin Hall effect of reflected light," *Opt. Lett.* **34**, 2551 (2009).
49. H. Luo, X. Zhou, W. Shu, S. Wen, and D. Fan, "Enhanced and switchable spin Hall effect of light near the Brewster angle on reflection," *Phys. Rev. A* **84**, 043806 (2011).
50. X. Ling, X. Zhou, X. Yi, W. Shu, Y. Liu, S. Chen, H. Luo, S. Wen, and D. Fan, "Giant photonic spin Hall effect in momentum space in a structured metamaterial with spatially varying birefringence," *Light Sci. Appl.* **4**, e290 (2015).